BEILSTEIN JOURNAL OF NANOTECHNOLOGY

Supporting Information

for

Solution combustion synthesis of a nanometer-scale Co_3O_4 anode material for Li-ion batteries

Monika Michalska, Huajun Xu, Qingmin Shan, Shiqiang Zhang, Yohan Dall'Agnese, Yu Gao, Amrita Jain and Marcin Krajewski

Beilstein J. Nanotechnol. **2021,** *12,* 424–431. doi:10.3762/bjnano.12.34

Additional data

Table S1: Comparison of the electrochemical performance of different Co_3O_4 powders applied as anode materials in Li-ion batteries (1 C = 890 mA·g^{-1}).

Synthesis method	**Powder shape**	**Charge-discharge rate (mA g^{-1})**	**Surface area (m^2 g^{-1})**	**Number of cycles**	**Specific capacity (mAh g^{-1})**	**Reference**
sol-gel	mesoporous octahedra	200	48.5	60	1195	[1]
sol-gel	agglomerated nanoparticle	178 (0.2 C)	–	over 120	620	[2]
sol-gel	bowl-like hollow microsphere	178 (0.2 C)	12.8	50	1441	[3]
electrospinning	microfiber	50	–	20	741	[4]
electrospinning	nanowire	222 (0.25 C)	68	60	805	[5]
electrospinning	nanotube	222 (0.25 C)	95	60	856	[5]
electrospinning	nanofiber	445 (0.5 C)	46.5	40	604	[6]
electrospinning	porous nanofiber	500	29.8	over 350	600	[7]
hydrothermal	microsphere	50	93.4	25	550	[8]
hydrothermal	nanowire array	500	–	100	1031	[9]
solution	nanocage	178 (0.2 C)	–	50	864	[10]
ammonia-assisted hydrothermal	snowflake-like nanosheet	500	22.5	100	1044	[11]
hydrothermal	mesoporous nanosheet	100	11.9	100	1067	[12]
hydrothermal	porous nanoplate	178 (0.2 C)	14.5	80	1001	[13]
hydrothermal	nanosphere	400	10.7	140	970	[14]
hydrothermal	nanocube	400	7	140	490	[14]
solvothermal	mesoporous hollow sphere	1500	23.9	90	1320	[15]
precipitation	nanoparticle	89 (0.1 C)	–	130	423	[16]
surfactant-assisted precipitation	nanowire	110	8	50	611	[17]
co-precipitation	flower-like nanoparticle	445 (0.5 C)	31.9	350	1227	[18]
alumina-temple	nanorod	50	–	100	815	[19]
alumina-temple	nanotube	50	–	100	850	[19]
alumina-temple	nanoparticle	50	–	100	830	[19]
thermal decomposition	nanocage	50	31.9	30	970	[20]
precipitation	nanooctahedra	100	–	200	956	[21]
ultrasonic spray pyrolysis	porous microsphere	400	43.3	50	654	[22]
spray drying	mesoporous nanosheet	3500	13	100	868	[23]
urea-assisted refluxing	hydrotalcite-like nanoparticle	100	22.4	100	741	[24]

Synthesis method	Powder shape	Charge-discharge rate (mA g^{-1})	Surface area (m^2 g^{-1})	Number of cycles	Specific capacity (mAh g^{-1})	Reference
microwave-assisted and urea-assisted hydrolysis	porous nanowire	400	41	100	600	[25]
surfactant-assisted self-assembly	nanosheet	100	94.3	30	1868.6	[26]
solution combustion	nanoflake	178	2.3	100	908	[27]
solution combustion	nanoparticle	100	3	100	1060	This work

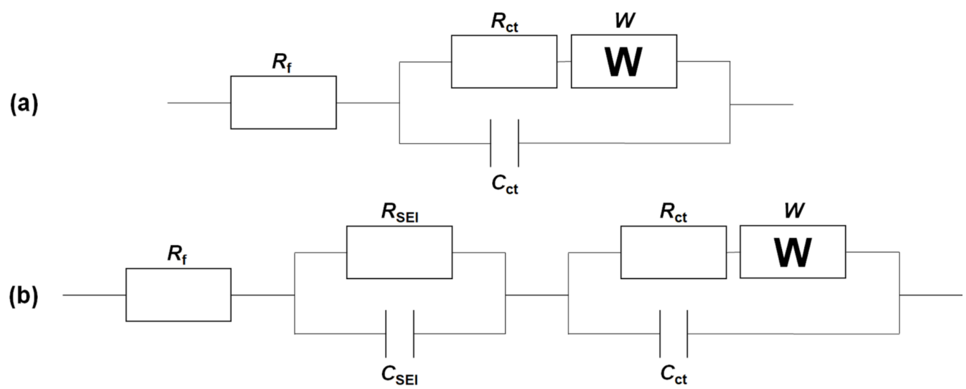

Figure S1: Equivalent circuit corresponding to the electrochemical impedance spectroscopy (EIS) measurements for the cell (a) before cycling, and (b) after cycling; R_f – contact resistance, R_{SEI} – the solid-electrolyte interface (SEI) resistance, C_{SEI} – the surface capacitance, R_{ct} – the charge transfer resistance at the electrode/electrolyte interface, C_{ct} – the double layer capacitance of the electrode, W – Warburg impedance.

References

1. Guo, J. X.; Chen, L.; Zhang, X.; Jiang, B.; Ma, L. Z. *Electrochim. Acta* **2014**, *129*, 410–415.

2. Devi, V. S.; Athika, M.; Duraisamy, E.; Prasath, A.; Sharma, A. S.; Elumalai, P. *J. Energy Storage* **2019**, *25*, 100815.

3. Wen, J. W.; Zhang, D. W.; Zang, Y.; Sun, X.; Cheng, B.; Ding, C. X.; Yu, Y.; Chen, C. H. *Electrochim. Acta* **2014**, *132*, 193–199.

4. Gu, Y. X.; Jian, F. F.; Wang, X. *Thin Solid Films* **2008**, *517*, 652–655.

5. Chen, M. H.; Xia, X. H.; Yin, J. H.; Chen, Q. G. *Electrochim. Acta* **2015**, *160*, 15–21.

6. Ding, Y. H.; Zhang, P.; Long, Z. L.; Jiang, Y.; Huang, J. N.; Yan, W. J.; Liu, G. *Mater. Lett.* **2008**, *62*, 3410–3412.

7. Fan, L.; Zhang, W. D.; Zhu, S. P.; Lu, Y. Y. *Ind. Eng. Chem. Res.* **2017**, *56*, 2046–2053.

8. Liu, Y.; Mi, C. H.; Su, L. H.; Zhang, X. G. *Electrochim. Acta* **2008**, *53*, 2507–2513.

9. Zhan, L.; Wang, S. Q.; Ding, L. X.; Li, Z.; Wang, H. H. *Electrochim. Acta* **2014**, *135*, 35–41.

10. Liu, D. Q.; Wang, X.; Wang, X. B.; Tian, W.; Bando, Y.; Goldberg, D. *Sci. Rep.* **2013**, *3*, 2543.

11. Wang, B.; Lu, X. Y.; Tang, Y. *J. Mater. Chem. A* **2015**, *3*, 9689–9699.

12. Wu, S. M.; Xia, T.; Wang, J. P.; Lu, F. F.; Xu, C. B.; Zhang, X. F.; Huo, L. H.; Zhao, H. *Appl. Surf. Sci.* **2017**, *406*, 46–55.

13. Liang, C. C.; Cheng, D. F.; Ding, S. J.; Zhao, P. F.; Zhao, M. S.; Song, X. P.; Wang, F. *J. Power Sources* **2014**, *251*, 351–356.

14. Zhang, B.; Zhang, Y. B.; Miao, Z. Z.; Wu, T. X.; Zhang, Z. D.; Yang, X. G. J*. Power Sources* **2014**, *248*, 289–295.

15. Shin, H.; Lee, W. J. *Mater. Chem. Phys.* **2018**, *214*, 165–171.

16. Subalakshimi, P.; Sivashanmugam, A. *ChemistrySelect* **2018**, *3*, 5040–5049.

17. Yao, X. Y.; Xin, X.; Zhang, Y. M.; Wang, J.; Liu, Z. P.; Xu, X. X. *J. Alloys Compd.* **2012**, *521*, 95–100.

18. Jadhav, H. S.; Rai, A. K.; Lee, J. Y.; Kim, J.; Park, C. J. *Electrochim. Acta* **2014**, *146*, 270–277.

19. Li, W. Y.; Xu, L. N.; Chen, J. *Adv. Funct. Mater.* **2005**, *15*, 851–857.
20. Yan, N.; Hu, L.; Li, Y.; Wang, Y.; Zhong, H.; Hu, X. Y.; Kong, X. K.; Chen, Q. W. *J. Phys. Chem. C* **2012**, *116*, 7227–7235.
21. Xu, G. L.; Li, J. T.; Huang, L.; Lin, W. F.; Sun, S. G. *Nano Energy* **2013**, *2*, 394–402.
22. Yin, X.; Wang, Z. X.; Wang, J. X.; Yan, G. C.; Xiong, X. H.; Li, X. H.; Guo, H. J. *Mater. Lett.* **2014**, *120*, 73–75.
23. Son, M. Y.; Kim, J. H.; Kang, Y. C. *Electrochim. Acta* **2014**, *116*, 44–50.
24. Lu, Z. P.; Ding, J. J.; Lin, X. H.; Liu, Y.; Ye, H. T.; Yang, G.; Yin, F.; Yan, B. *Powder Technol.* **2017**, *309*, 22–30.
25. Wang, J. Q.; Niu, B.; Du, G. D.; Zeng, R.; Chen, Z. X.; Guo, Z. P.; Dou, S. X. *Mater. Chem. Phys.* **2011**, *126*, 747–754.
26. Yang, J.; Gao, M. Z.; Lei, J. F.; Jin, X. J.; Yu, L.; Ren, F. F. *J. Solid State Chem.* **2019**, *274*, 124–133.
27. Wen, J. W.; Xu, L.; Wang, J. X.; Xiong, Y.; Ma, J. J.; Jiang, C. R.; Cao, L. H.; Li, J.; Zeng, M. *J. Power Sources* **2020**, *474*, 228491.